Interfacial disorder and optoelectronic properties of diamond nanocrystals

G. Vantarakis,[1,2] C. Mathioudakis,[2] G. Kopidakis,[2] C. Z. Wang,[3] K. M. Ho,[3] and P. C. Kelires[1,4,*]
[1]*Department of Mechanical and Materials Science Engineering, Cyprus University of Technology, P.O. Box 50329, 3603 Limassol, Cyprus*
[2]*Department of Materials Science and Technology, University of Crete, P.O. Box 2208, 71003 Heraklion, Crete, Greece*
[3]*Department of Physics and Ames Laboratory, Iowa State University, Ames, Iowa 50011, USA*
[4]*Department of Physics, University of Crete, P.O. Box 2208, 710 03 Heraclion, Crete, Greece*
(Received 1 May 2009; published 7 July 2009)

We present in this work a theoretical framework based on the tight-binding method, which is able to probe at a local atomic level the optoelectronic response of nanomaterial systems and link it to the associated disorder. We apply this methodology to carbon nanocomposites containing diamond nanocrystals. We find that significant structural and topological disorder exists at the interface between the nanodiamonds and the embedding amorphous carbon matrix. This can be quantitatively probed by extracting the Urbach energies from the optical parameters. Disorder in the nanocrystals appears in their outer shell near the interface and is manifested as bond length and angle distortions. Energetics and stability analysis show that nanodiamonds embedded in matrices with high density and high fraction of fourfold coordinated atoms are more stable.

DOI: 10.1103/PhysRevB.80.045307 PACS number(s): 78.66.Sq, 71.15.Pd, 68.35.Ct

I. INTRODUCTION

One of the prominent issues in the physics of nanocomposite and nanostructured materials is the influence of the interfacial structure on their mechanical and optoelectronic properties. At the interface between an embedded nanostructure and the host material, several structural modifications take place due to size and/or chemical mismatch of the constituent phases. The associated distortions and disorder may have a substantial effect on the nanostructured material's response. Disorder at the interface can take various forms. It can be *structural*, related to intrinsic defects (miscoordinated atoms) and distortions in bond angles and lengths, or *topological*, related to the distribution and clustering of various kinds of bonds and hybrids.[1,2] For example, defects, bond distortions, and oxygen bonds at the interface are believed to strongly influence the gap of Si nanocrystals in amorphous silica.[3,4]

Probing the effects of certain interfacial elements of disorder, such as defects and wrong bonds, is possible through various experimental and theoretical techniques. However, the quantitative analysis and decomposition of the overall interfacial disorder into contributions from the constituent phases is a much more involved and tedious procedure. It requires the ability to probe at a local atomic level the mechanical or optoelectronic response of the nanomaterial and link it to the associated disorder.

We present in this work a theoretical framework, which is able to achieve this goal. Methods based on empirical interatomic potentials have the capability to probe locally the structure, but are not so accurate and cannot yield optoelectronic properties. First-principles methods, on the other hand, while accurate, are computationally very demanding, and cannot decompose locally the energy and the optical parameters of a system. We therefore rely on a state-of-the-art tight-binding (TB) method which is accurate and transferable, not so computationally demanding as *ab initio* methods, thus making the problem tractable, and which gives us the opportunity to probe locally both the interfacial disorder and the optical constants of a nanomaterial.

We apply our methodology to nanodiamond carbon, a nanostructured two-phase carbon material, denoted as n-D/a-C, which is composed of diamond nanocrystals embedded in amorphous carbon matrix.[5–7] The embedding in a rigid matrix is expected to have certain advantages, at least for the mechanical properties. We have recently shown[7] that this nanomaterial, for high-enough density of embedded nanodiamonds, has excellent mechanical properties exhibiting improved elastic behavior over single-phase tetrahedral amorphous carbon (*ta*-C),[1] while retaining high hardness and fracture strength, making it highly suitable for applications in microelectromechanical devices. Here, we focus on the optoelectronic properties of this material, especially on how disorder affects these properties and in what degree nanoinclusions can tailor the properties of *ta*-C.

The essence of our approach lies in the extraction of the absorption coefficient and the optical gaps from the calculated dielectric function of the nanomaterial, and the decomposition of these quantities into contributions from atoms at the interface, the core of the nanoinclusions, and the amorphous matrix (AM). Central to our analysis is the utilization of the concept of Urbach energy, E_U, to probe the disorder at the interface. E_U has been shown to be an excellent probe of disorder in a-Si:H,[8] especially regarding intrinsic defects. We show here that E_U is as well an excellent probe of disorder in nanostructured carbon, providing information on defects, clustered sp^2 and sp^3 atoms, and bond distortions.

The paper is organized as follows. In Sec. II, the tight-binding method used and the methodology to extract the optical parameters are described. In Sec. III, the results and the associated discussion are given. Conclusions and prospects for extending our approach to other carbon nanomaterials are discussed in Sec. IV.

II. METHODOLOGY

A. Energetics, simulations, and computational cells

We treat the interatomic interactions in the nanostructured networks using the tight-binding method. This bridges the

gap between classical and first-principles calculations. It is more accurate and transferable than empirical schemes because it provides a quantum-mechanical description of the interactions. On the other hand, while less accurate than *ab initio* approaches, it yields greater statistical precision and allows the use of larger cells, which compensate in part the sacrifice in accuracy.

In the present case, we use the environment-dependent tight-binding (EDTB) model of Tang *et al.*[9] This model goes beyond the traditional two-center approximation and allows the TB parameters to change according to the bonding environment. Compared to the previous two-center model developed earlier by the same group,[10–12] the EDTB model improves accuracy and transferability. In a recent study,[13] the method was shown to successfully describe the variation in sp^3 bonding with density and of the bulk modulus with sp^3 fraction in *a*-C, through the entire range of possible densities. It was also recently used[14] to study some basic optoelectronic properties of *a*-C, i.e., the electronic density of states (EDOS) and the complex dielectric function. The results compared favorably with experiment.[15] In particular, the positions of the main peaks in the imaginary part of the dielectric function due to the π-π^* transitions (at $\sim$3 eV), due to the σ-σ^* transitions (at $\sim$10 eV), as well as the shift in the σ-σ^* peak to higher energies with increasing sp^2 fraction, were correctly reproduced. In a subsequent study,[2] the optical gaps, the absorption coefficient, and Urbach energies of *a*-C were extracted. Having established its reliability, the EDTB model is now applied to the more involved nanocomposite case.

To generate and equilibrate the nanostructured networks, tight-binding molecular-dynamics (TBMD) simulations were carried out in the canonical (N,V,T) ensemble, in which equilibration of a given structure is performed under conditions of constant number of atoms N, constant volume V, and constant temperature T in the system. T is controlled via a usual stochastic temperature control algorithm.[16] The embedded nanostructures are formed by initially melting crystalline diamond structures and subsequently quenching them, while keeping a certain number of atoms in the central region of the cells within a spherical volume of predetermined radius frozen in their ideal crystal positions. Melting was done at 6000 K and typical quenching durations and rates used are 40 ps and 300 K/ps, respectively. Periodic boundary conditions (PBC) are applied to our cubic computational cells, which consist of a total of 512 atoms, with the number of atoms in the nanodiamonds ranging from 100 to 200. The use of PBC makes the problem equivalent to simulating an infinite array of well-ordered nanocrystals in *a*-C. After quenching to 300 K, which produces amorphization of the matrix surrounding the nanocrystals, the cells are thoroughly relaxed with respect to atom positions and densities. Relaxations are particularly important at the interface region, where the crystallites mainly adjust to the host environment. Cells with varying coordinations (densities) of the amorphous matrix can be formed by appropriately choosing the initial density (volume) of the cells. The nanocrystal size is controlled by the number of shells kept frozen during quenching. Finally, the cells are cooled down to 0 K where properties are taken.

As a benchmark, we use the properties of the Wooten-Winer-Waire (WWW) model[17] of *a*-C, which is a hypothetical model of "amorphous diamond" (*a*-D), completely tetrahedral and constructed from the diamond lattice by a bond-switching mechanism. We used the 512-atom cell constructed by Djordjević, Thorpe, and Wooten.[18] We relaxed its topology and density with the EDTB model. The cell remains perfectly tetrahedral. The WWW model, although hypothetical, is very useful because it provides an upper bound to the density, sp^3 fraction, and optical gap of *a*-C, and so can be compared to both the amorphous matrix and the nanodiamonds in the nanomaterial.

B. Formalism for optical parameters and disorder

Our studies focus on the investigation of the optoelectronic properties and the link to the disorder at the interface. So, the most important ingredient in our approach is the decomposition and analysis of the electronic and optical parameters of the system into contributions from atoms in the amorphous matrix and the nanodiamonds, and from the various carbon hybrids. This is achieved by analyzing the TB wave functions and the associated optical matrix elements into the respective contributions. The local nature of the atomic orbitals in the expansion of the wave function allows the identification of the contributions from individual atomic sites.

While the extraction of the electronic structure from the TB wave functions and eigenvalues is a straightforward procedure, it is not so for the optical properties since it involves certain approximations. The central source of information for the optical properties is the complex dielectric function, $\epsilon=\epsilon_1+i\epsilon_2$, expressed in terms of its real and imaginary parts, $\epsilon_1=n^2-k^2$ and $\epsilon_2=2nk$, where n and k are the refractive index and the extinction coefficient, respectively.

We first calculate the imaginary part ϵ_2, which is directly correlated with the electronic structure of the material and is defined as

$$\epsilon_2(E)=\frac{2}{V}\left(\frac{2\pi\hbar e}{mE}\right)^2\sum_{i,f}|\langle f|\vec{P}|i\rangle|^2\delta(E_f-E_i-E), \qquad (1)$$

where the matrix elements show the electronic transitions from an initial occupied state to a final unoccupied state. $\vec{P}$ is the momentum operator, E_i and E_f are the energy eigenvalues of the initial (valence) and final (conduction) states, E is the photon energy, V is the volume of the cell, and the sum is over all initial and final eigenstates. A crucial step is in the evaluation of the momentum matrix elements $\langle f|\vec{P}|i\rangle$, which cannot be calculated directly. We bypass this obstacle by extracting them from the position matrix elements using the approximation[19]

$$\hbar\langle f|\vec{P}|i\rangle=im(E_f-E_i)\langle f|\vec{r}|i\rangle. \qquad (2)$$

Figure 1 shows the calculated ϵ_2 for diamond, comparing favorably to experiment,[1] and for *a*-D.

As it is customary for amorphous and disordered semiconductors, where a true gap cannot be formally defined, the Tauc and the E_{04} optical gaps are used to define the mini-

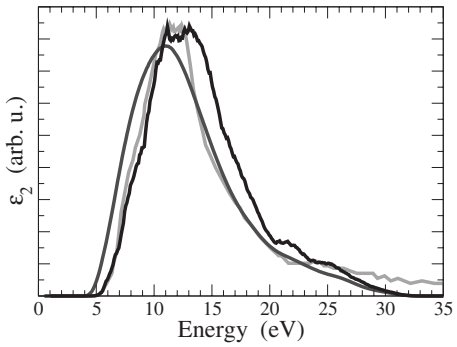

FIG. 1. Calculated imaginary part of the dielectric function of Diamond (dark line) and amorphous diamond (gray line), compared to an experimentally derived function (Ref. 1) for diamond (light gray line).

mum separation between occupied and unoccupied states. These are the optical gaps used here to also describe the nanostructured carbon materials. The Tauc gap E_T is determined by plotting the quantity $E\sqrt{\epsilon_2}$ versus photon energy E and extrapolating the linear plots to the energy axis. This is demonstrated for a-D in Fig. 2(a). The calculated Tauc gap is ~5 eV, compared to 5.5 eV for diamond with the EDTB model.

On the other hand, the E_{04} optical gap is defined as the energy at which the absorption coefficient

$$\alpha(E) = \frac{E\epsilon_2(E)}{\hbar nc} \tag{3}$$

reaches the value 10^4 cm^{-1}. This requires the knowledge of the refractive index n. We extract n by solving the system of equations defining ϵ_1 and ϵ_2. (For this, the ϵ_1 is calculated from ϵ_2 through the Kramers-Kronig dispersion relation and the extinction coefficient k is eliminated). Figure 2(b) demonstrates the estimation of E_{04} from $\alpha(E)$ for a-D. It is found to be ~4.5 eV, somewhat lower than the Tauc gap. This is a systematic trend in amorphous semiconductors.

To link disorder and optical parameters, we use the concept of Urbach energy E_U, whose values and variations reflect the disorder in a network arising from both structural and topological distortions and from defects.[2] E_U is customarily defined as the inverse of the local slope of $\ln[\alpha(E)]$ at the E_{03} photon energy, i.e., when $\alpha(E)$ takes the value 10^3 cm^{-1},[1,8]

$$E_U^{-1} = \frac{d\ln[\alpha(E_{03})]}{dE}. \tag{4}$$

So, it captures quantitatively the variations in $\alpha(E)$ deep within the gap, below $\alpha(E)=10^4$ cm^{-1}. These variations are associated to disorder-induced changes and to defects. Figure 2(b) demonstrates the extraction of E_U from the calculated $\alpha(E)$ for a-D. Its value is ~0.9, *it is not zero*. Taking into account that there are no sp^2 sites and defects in the fully tetrahedral network, this shows clearly that the *inherent* structural disorder (distortions in bond angles and lengths, and in dihedral angles) contributes to E_U.

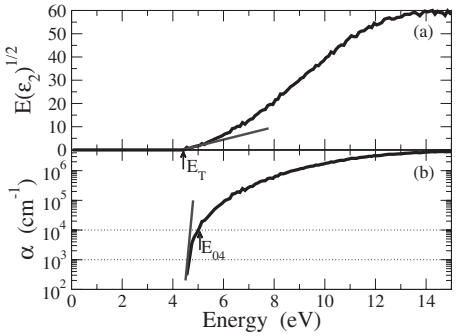

FIG. 2. (a) Calculation (extraction) of the Tauc gap of amorphous diamond from the imaginary part of the dielectric function. (b) Calculation (extraction) of the E_{04} gap and the Urbach energy E_U of amorphous diamond from the absorption coefficient.

TABLE I. Nanodiamond volume fraction and sp^3 fraction in the embedding AM, density of AM, total energy per atom, and nanodiamond formation energy of six representative n-D/a-C networks.

Network	n-D V.F (%)	sp^3_{AM} (%)	ρ_{AM} (g/cm^3)	E_{tot}/atom (eV)	E_{form}/atom (eV)
A	48.8	88	3.24	−7.13	0.006
B	12.0	88	3.24	−6.94	0.025
C	20.8	81	3.06	−6.96	0.040
D	8.7	71	2.91	−6.81	0.098
E	3.8	65	2.77	−6.73	0.146
F	6.24	51	2.58	−6.73	0.135

III. RESULTS AND DISCUSSION

We first begin with a description of the energetics and microstructure of n-D/a-C networks. Structural data of six representative networks, produced by TBMD simulations as described in the previous section, are given in Table I. They range in density and sp^3 fraction of the embedding matrix, and in the volume fraction occupied by the nanocrystals, and thus in their sizes. Two clear trends are extracted from these data. The first is the well-known linear dependence between density and sp^3 fraction in the amorphous matrix.[1,13] The second regards the behavior of the *formation energy* of a nanocrystal in the AM. This is given by

$$E_{form} = E_{total} - N_a E_a - N_c E_c, \tag{5}$$

where E_{total} is the total cohesive energy of the composite system (amorphous matrix plus nanocrystal), E_c is the cohesive energy per atom of the respective crystalline phase, N_c is the number of atoms in the nanocrystal, N_a is the number of atoms in the amorphous matrix, and E_a is the cohesive energy per atom of the pure, undistorted amorphous phase (without the nanocrystal) with coordination z_{am}. The results show that E_{form} gets smaller as the matrix becomes more dense and rigid (increasing z_{am}), or as the volume fraction (size) of the nanocrystal increases. This indicates increased stability, and it is in accord with previous Monte Carlo simulations based on empirical interactions.[6] For example, let us

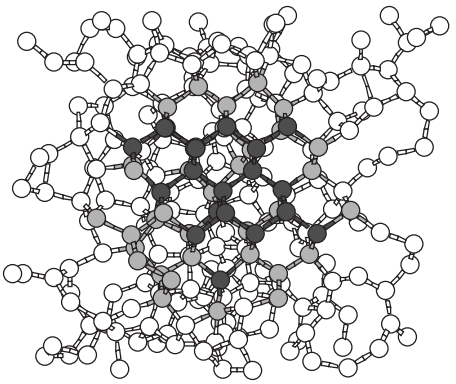

FIG. 3. Ball-and-stick model (crossview) of a representative nanocomposite network of 512 atoms under periodic boundary conditions composed of a nanodiamond particle occupying a volume fraction of 9% inside an *a*-C matrix with a density of 2.96 g cm^{-3}. Open spheres denote atoms in the AM. Dark spheres show the undistorted atoms in the core of the nanodiamond. Light gray spheres denote nanodiamond atoms at the interface with distorted geometry.

compare networks A and B: they have the same density and sp^3 fraction in the matrix, but A has lower formation energy because the nanocrystal is bigger (occupies larger volume in the system). For such sizes and matrix properties, as in network A, the formation energy of nanocrystals is very small.

Figure 3 illustrates a representative 512-atom cell in a ball-and-stick fashion. Since we are interested in the disorder induced by the embedding, we distinguish between those atoms in the nanocrystal, which retain their "crystallinity" and those that are substantially disordered. Deviations from tetrahedral arrangement are detected by calculating the magnitude of the tetrahedral vector $\vec{v}_t$, which equals to the sum of the vectors pointing from an atom to its nearest neighbors and it is zero for perfect arrangement. This analysis shows clearly that several atoms at the interface of the nanocrystal with the matrix are subjected to deformations. This is the result of the incompatibility of the ordered crystalline phase inside the fully disordered amorphous matrix, which is reflected in both the density gradients between the two phases and the loss of bond directionality across the interface. Our main aim in this paper is to unravel how these local, at the atomic level, deformations influence the optoelectronic properties.

The electronic structure of representative *n*-D/*a*-C networks, as described by the electronic density of states, is shown in Fig. 4. The EDOS was extracted from the TB wave functions and was analyzed in contributions from the atoms in the nanocrystals and in the amorphous matrix. (The local nature of atomic orbitals, in which the wave function is expanded, permits this analysis.) It is clear from the graphs, and rather expected, that the main contribution to the formation of the gap (absence of electronic states) and of any states located in the gap region comes from the AM, as this has lower energy gap than diamond due to the presence of sp^2 hybrids. The shrinking of the gap region shown in the graphs is a result of the progressive increase in sp^2 hybrids in the networks, which control the gap through the separation of π-π^* bonding-antibonding states. Further analysis shows

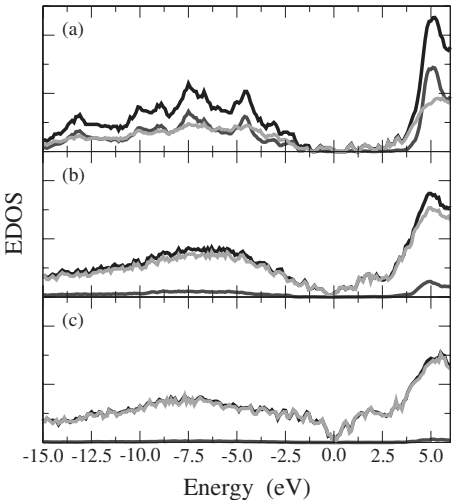

FIG. 4. EDOS of representative nanocomposite networks with (a) 88% and 3.24 g cm^{-3}, (b) 71% and 2.91 g cm^{-3}, and (c) 51% and 2.58 g cm^{-3} sp^3 fractions and densities, respectively. The dark line shows the total function, while the gray and light gray lines refer to the *n*-D and AM-projected contributions, respectively. The Fermi level is at 0 eV.

that a smaller contribution to the gap states originates from distorted sp^3 atoms of the nanocrystals at the interface. This subtle effect will be analyzed in detail below.

In the next step, we calculate the dielectric function of our nanocomposite networks. The calculated ϵ_2 functions for our representative networks are shown in Fig. 5. Again, analysis of the total function into contributions from the atoms in the nanocrystals and in the amorphous matrix was done. It can be seen that the optical response of the nanocomposite system is progressively varied, as the sp^2 fraction in the AM is increased from having nearly diamondlike nature [network in panel (a), domination of nanodiamond's contribution] to having nearly graphitelike nature [network in panel (c), domina-

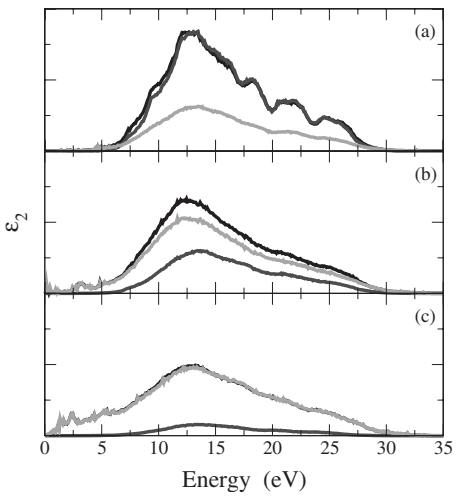

FIG. 5. Calculated imaginary part of the dielectric function of the representative nanocomposite networks, whose EDOS is shown in Fig. 4. The dark line shows the total function, while the gray and light gray lines refer to the *n*-D and AM-projected contributions, respectively.

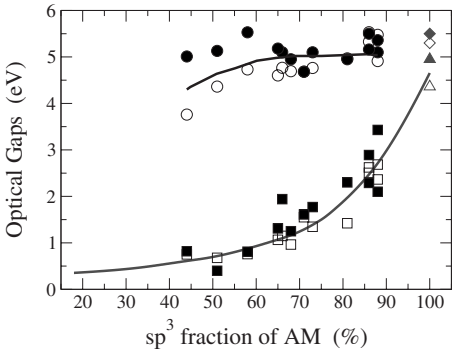

FIG. 6. Variation in optical gaps of n-D/a-C networks as a function of sp^3 fraction in the AM. Circles and squares indicate the n-D and AM contributions, respectively. Diamonds and triangles show the values for diamond and amorphous diamond. Filled symbols are for the E_{04} gaps and open symbols for the Tauc gaps. Grey line shows for comparison the variation in optical gaps in pure a-C.

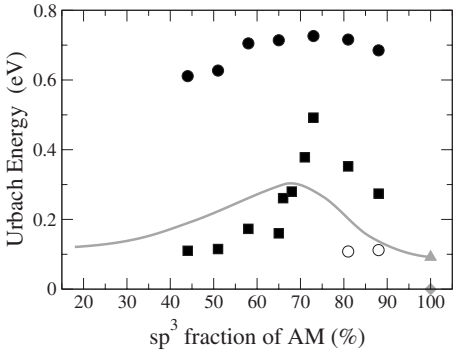

FIG. 7. Variation in the Urbach energy in n-D/a-C networks as a function of sp^3 fraction in the AM. Filled circles and squares indicate the n-D and AM contributions, respectively. Open circles show values from core atoms in the n-D. Diamond and triangle show the values for diamond and amorphous diamond, respectively. Light gray line shows for comparison the variation in Urbach energies in pure a-C.

tion of the AM]. It is also clear that the energy gaps (absence of electronic transitions at the edge of the spectra) are reduced as the sp^2 fraction increases, and that near the gap the main contribution comes from transitions between states localized at atoms in the AM.

Following the procedure described in the previous section, we now investigate and analyze more quantitatively and in detail the optical gap of nanocomposite n-D/a-C by calculating the Tauc and E_{04} gaps. The variation in both gaps as a function of sp^3 fraction in the AM is shown in Fig. 6. The respective variation in the case of the single-phase amorphous carbon system, as calculated in Ref. 3, is also given for comparison. The central characteristic in this variation is that the gap is rapidly increasing when the sp^3 fraction exceeds 70%, which defines the region of tetrahedral amorphous carbon. Amorphous diamond has a gap close but lower than diamond.

It is interesting to examine whether the existence of nanodiamonds increases the optical gap, for a given percentage of sp^3 hybrids in the AM, as compared to the single-phase amorphous system. For this purpose, we separated the contributions to the gaps from the atoms in the nanocrystals and the AM. We clearly observe that the contribution from the atoms in the AM follows qualitatively and quantitatively the variation in the gap of the pure system, with a slight increase in the tetrahedral region. On the other hand, the atoms in the nanocrystals contribute large gap values, around 5 eV, characteristic of amorphous diamond, but lower than crystalline diamond. The lower values are found in cases where the nanodiamonds are embedded in matrices rich in sp^2 hybrids. Given that the optical gap of the nanocomposite system is determined by the contribution of the component with the smaller gap, we conclude that the existence of nanodiamonds is expected to enhance the gap in cases of nanocomposites with large densities of nanodiamonds and high fraction of sp^3 hybrids in the AM.

A most interesting issue dealt with in this paper is the association of optical properties with the disorder in the system. This was achieved, as explained in detail in the methodology section, by using the tool of Urbach energy, E_U, whose variations are related in general to structural and topological disorders and to defects in a crystalline or amorphous network. The calculations of this quantity for the nanocomposite system are summarized in Fig. 7, together with the variation in E_U in the single-phase amorphous system.[2] The important result in the case of single-phase a-C is the nonmonotonic variation in E_U. This behavior can in short be explained as follows: if we exclude for the moment the contribution from defects (mainly unpaired sp^2 sites), the disorder in the network is generated upon embedding "minority" configurations into a host "majority" phase. Such configurations can be clusters or chains of sp^2 atoms inside an embedding high-density phase of sp^3 atoms, or clusters of sp^3 atoms embedded in a low-density sp^2 phase. In both cases, the incompatibility due to the substantially different geometries, effective atomic volumes, and local electronic structures of sp^3 and sp^2 hybrids produces disorder, which is both topological (associated to the size distribution of chains and clusters) and structural (associated to distortions in bond angles and lengths). The contribution to these two forms of disorder from the two regions, the one rich and the other poor in sp^3 atoms, creates the nonmonotonic variation with a maximum in Urbach energy somewhere in between the networks with high and low densities.

In the case of nanocomposite a-C, we observe a similar nonmonotonic variation in E_U, which comes from the atoms in the AM, but with higher values at the maximum of the variation and at the tetrahedral region. This indicates that excess disorder is produced on the atoms of the AM due to the embedding of the nanodiamonds. Somewhat smaller than single phase, values are calculated for low-density matrices, which can be explained by noting that the "minority" sp^3 configurations in the nanocomposite are now largely clustered (the nanodiamond), relieving part of the topological disorder (smaller number of clusters) in the matrix. At the tetrahedral region, the excess disorder in the matrix is attributed to increased clustering of sp^2 sites (topological disorder), in response to nanodiamond's embedding, and not to excess structural disorder, since incompatibility between the

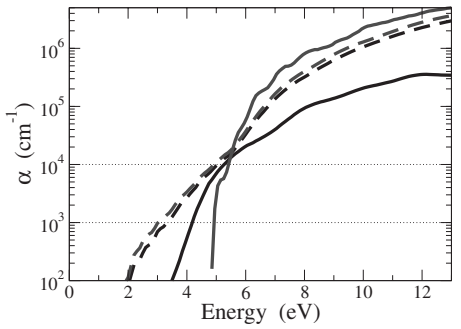

FIG. 8. Breakdown of the absorption coefficient (dashed gray line) of a network with 88% sp^3 fraction and 3.24 g cm^{-3} in the AM into contributions from n-D atoms at the core (dark solid line) and the interface (dark dashed line). For comparison, solid gray line indicates the calculated absorption of diamond.

nanodiamond and the sp^3-rich embedding matrix is low. Respectively, we observe quite high values of E_U contributed by atoms in the nanocrystals. If we combine this result with the previous finding that the optical gap of nanodiamonds is smaller than crystalline diamond's, we conclude that significant disorder is produced in the nanostructures due to their embedding in the AM. E_U is found to be more or less constant in the nanodiamonds studied, having a value around 0.6 to 0.7. It is logical to assume that the disorder originates from the interfacial region between the crystalline and the amorphous phases, and that there is a limit in the relaxation of distorted geometries in this region.

In order to investigate this issue, we analyzed the Urbach energy in the nanodiamonds into atomic contributions. This is done by calculating separately the absorption coefficient for atoms in the inner nucleus of the nanocrystals and for atoms close to the interface, and extracting the respective E_U. The results for $\alpha(E)$ from a typical case are shown in Fig. 8. It is clearly seen that the variation in the total absorption coefficient nearly coincides with the contribution from the atoms at the interface, while the absorption from the nucleus of n-D approaches the absorption of crystalline diamond. Therefore, the atoms at the interface are those which determine the Urbach energy for the whole nanocrystal. Such deformed atoms are the ones shown explicitly in Fig. 3. The disorder at the interior of the nanodiamonds is very small, since E_U is on the order of 0.1 eV, and it is constant as a function of sp^3 fraction in the AM.

Another issue concerns the relative contributions to E_U from the hybrid states in the nanocomposite system. Regarding the nanodiamond component, E_U comes of course solely from distorted sp^3 sites. The AM has a twofold contribution. The major part originates from π-π^* transitions, since E_U in a-C describes transitions between localized states. (It is well established that π states in a-C are strongly localized).[2,20] There is also a contribution from localized σ states. These originate from distorted sp^3 hybrids and are found to be localized at energies where the π and π^* peaks are located, well inside the σ-σ^* gap, and thus lie at the Urbach edge.

Finally, we examined the effect of few unpaired sp^2 sites in the AM component at the interfacial region on the optical transitions. For this, we calculated the absorption coefficient by excluding the contribution of states localized on such defects. The results show that the effect on both the E_{04} and E_U is small, indicating that transitions between states localized on unpaired sp^2 sites or between such states and neighboring π and σ states are negligible. This is in contrast to a-Si:H, where the spin density due to dangling bonds is a major factor in shaping up the Urbach edge. A similar result was found in the case of the pure a-C system.[2]

IV. SUMMARY/CONCLUSIONS

We have presented in this paper a theoretical framework, which can probe at a local atomic level the optoelectronic response of nanomaterial systems and link it to the associated disorder. Our approach is based on accurate TBMD calculations, which give us the opportunity to analyze locally both the interfacial disorder and the optical constants of a nanomaterial.

The method is applied to nanodiamond carbon, a nanostructured two-phase carbon material composed of diamond nanocrystals embedded in amorphous carbon matrix. We first examined the structure at the interface and found in all cases a shell of nanocrystal atoms that are substantially deformed. The stability analysis shows that larger nanodiamonds embedded in rigid matrices with high sp^3 fraction and density are more stable. We then analyzed the optoelectronic properties of the nanocomposite systems. The matrix has a dominant role in forming both the EDOS and the dielectric function, but with increasing sp^3 fraction and density nanodiamond contributions become substantial and are expected to enhance diamondlike behavior at the highly tetrahedral region. The Urbach energy E_U is shown to be a reliable probe of disorder in the system, linked directly with the optical response, and to provide information about disorder at the local level. Analysis of E_U into atomic contributions confirms that much of the disorder in the nanocrystals comes from the interface region. Defects at the interface (unpaired sp^2 sites and dangling bonds) are found to contribute negligibly to the optical transitions and the Urbach edge.

We are currently in the process to apply this methodology to other nanostructured carbon systems such as ultrananocrystalline diamond, embedded nanotubes, and nanofoams. Disorder in the grain boundaries, in the former case, and at interfaces with the embedding medium, in the latter cases, are far from being well understood.

ACKNOWLEDGMENTS

This work was supported by the Research Promotion Foundation of the Republic of Cyprus through the Grant No. EPYNE/0506/05. Ames Laboratory is operated for the U.S. Department of Energy by Iowa State University under Contract No. W-7405-Eng-82. This work was also supported by the Director for Energy Research, Office of Basic Energy Sciences.

*Author to whom correspondence should be addressed; pantelis.kelires@cut.ac.cy; kelires@physics.uoc.gr

[1] J. Robertson, Mater. Sci. Eng. R. **37**, 129 (2002).
[2] C. Mathioudakis, G. Kopidakis, P. Patsalas, and P. C. Kelires, Diamond Relat. Mater. **16**, 1788 (2007).
[3] M. V. Wolkin, J. Jorne, P. M. Fauchet, G. Allan, and C. Delerue, Phys. Rev. Lett. **82**, 197 (1999).
[4] G. Hadjisavvas and P. C. Kelires, Phys. Rev. Lett. **93**, 226104 (2004); Physica E **38**, 99 (2007).
[5] Y. Lifshitz, T. Kohler, T. Frauenheim, I. Guzmann, A. Hoffman, R. Q. Zhang, X. T. Zhou, and S. T. Lee, Science **297**, 1531 (2002); X. T. Zhou, Q. Li, F. Y. Meng, I. Bello, C. S. Lee, S. T. Lee, and Y. Lifshitz, Appl. Phys. Lett. **80**, 3307 (2002); Y. Yao, M. Y. Liao, T. Kohler, T. Frauenheim, R. Q. Zhang, Z. G. Wang, Y. Lifshitz, and S. T. Lee, Phys. Rev. B **72**, 035402 (2005).
[6] M. G. Fyta, I. N. Remediakis, and P. C. Kelires, Phys. Rev. B **67**, 035423 (2003).
[7] M. G. Fyta, I. N. Remediakis, P. C. Kelires, and D. A. Papaconstantopoulos, Phys. Rev. Lett. **96**, 185503 (2006).
[8] R. A. Street, *Hydrogenated Amorphous Silicon* (Cambridge University, New York, 1991).
[9] M. S. Tang, C. Z. Wang, C. T. Chan, and K. M. Ho, Phys. Rev. B **53**, 979 (1996).
[10] C. H. Xu, C. Z. Wang, C. T. Chan, and K. M. Ho, J. Phys.: Condens. Matter **4**, 6047 (1992).
[11] C. Z. Wang and K. M. Ho, Phys. Rev. Lett. **71**, 1184 (1993).
[12] G. Kopidakis, C. Z. Wang, C. M. Soukoulis, and K. M. Ho, Phys. Rev. B **58**, 14106 (1998).
[13] C. Mathioudakis, G. Kopidakis, P. C. Kelires, C. Z. Wang, and K. M. Ho, Phys. Rev. B **70**, 125202 (2004).
[14] C. Mathioudakis, G. Kopidakis, P. C. Kelires, P. Patsalas, M. Gioti, and S. Logothetidis, Thin Solid Films **482**, 151 (2005).
[15] S. Waidmann, M. Knupfer, J. Fink, B. Kleinsorge, and J. Robertson, J. Appl. Phys. **89**, 3783 (2001).
[16] S. Nosé, Mol. Phys. **52**, 255 (1984); J. Chem. Phys. **81**, 511 (1984).
[17] F. Wooten, K. Winer, and D. Weaire, Phys. Rev. Lett. **54**, 1392 (1985).
[18] B. R. Djordjević, M. F. Thorpe, and F. Wooten, Phys. Rev. B **52**, 5685 (1995).
[19] W. A. Harrison, *Elementary Electronic Structure* (World Scientific, Singapore, 1999), p. 219.
[20] C. W. Chen and J. Robertson, J. Non-Cryst. Solids **227-230**, 602 (1998).